Applied Microbiology and Biotechnology (2022) 106:2063–2077
https://doi.org/10.1007/s00253-022-11848-8

APPLIED GENETICS AND MOLECULAR BIOTECHNOLOGY

Coordinate regulation of carbohydrate metabolism and virulence by PtsH in pathogen *Edwardsiella piscicida*

Qiaoqiao Mao[1] · Jihao Jiang[1] · Xiao Wu[1] · Rongjing Xu[2] · Yue Ma[1,3] · Yuanxing Zhang[4,3] · Shuai Shao[1,3] · Qiyao Wang[1,3]

Received: 6 February 2022 / Revised: 16 February 2022 / Accepted: 20 February 2022 / Published online: 26 February 2022

Abstract

Carbohydrate metabolism of bacterial pathogens conducts crucial roles in regulating pathogenesis but the molecular mechanisms by which metabolisms and virulence are been modulated and coordinated remain to be illuminated. Here, we investigated in this regard *Edwardsiella piscicida*, a notorious zoonotic pathogen previously named *E. tarda* that could ferment very few PTS sugars including glucose, fructose, mannose, N-acetylglucosamine, and N-acetylgalactosamine. We systematically characterized the roles of each of the predicted 23 components of phosphotransferase system (PTS) with the respective in-frame deletion mutants and defined medium containing specific PTS sugar. In addition, PtsH was identified as the crucial PTS component potentiating the utilization of all the tested PTS sugars. Intriguingly, we also found that PtsH while not Fpr was involved in T3SS gene expression and was essential for the pathogenesis of *E. piscicida*. To corroborate this, His15 and Ser46, the two established PtsH residues involved in phosphorylation cascade, showed redundant roles in regulating T3SS yields. Moreover, PtsH was shown to facilitate mannose uptake and transform it into mannose-6-phosphate, an allosteric substrate established to activate EvrA to augment bacterial virulence. Collectively, our observations provide new insights into the roles of PTS reciprocally regulating carbohydrate metabolism and virulence gene expression.

Key points

- *PTS components' roles for sugar uptake are systematically determined in Edwardsiella piscicida.*
- *PtsH is involved in saccharides uptake and in the regulation of E. piscicida's T3SS expression.*
- *PtsH phosphorylation at His15 and Ser46 is essential for the T3SS expression and virulence.*

Keywords *Edwardsiella piscicida* · Mannose · Phosphotransferase system · Type III secretion system (T3SS) · Virulence

Introduction

Bacteria show high metabolic versatility towards carbon sources for survival and adaptation in continuously changing environments. Various transportation systems are equipped in bacteria to cope with sugar specificities for saccharides utilizing ATP, ion gradients, and phosphoenolpyruvate as energy sources. Phosphoenolpyruvate carbohydrate phosphotransferase system (PTS) is a multi-functional system in a diverse array of bacteria and plays pivotal roles in saccharides uptake (Jeckelmann and Erni 2019, 2020; Galinier and Deutscher 2017). During the utilization of distinct sugars, the phosphorylation state of carbohydrates would be modified by cognate PTS components before being delivered into the cytoplasm, which is varied respectively to PTS sugars and the metabolic state of the cell.

Conventionally, PTS contains two general components, enzyme I (EI) and the histidine-containing phosphocarrier protein (HPr), as well as sugar-specific enzyme II (EII) complexes. EII family proteins consist of EII A/B/C/D subfamilies and EII D only appear in the PTS-mannose family (Stolz et al. 1993; Liu et al. 2019). In response to the availability of specific

✉ Shuai Shao
shaoscott@163.com

[1] State Key Laboratory of Bioreactor Engineering, East China University of Science and Technology, Shanghai 200237, China

[2] Yantai Tianyuan Aquatic Co. Ltd, Yantai, Shandong, China

[3] Shanghai Engineering Research Center of Maricultured Animal Vaccines, Shanghai 200237, China

[4] Southern Marine Science and Engineering Guangdong Laboratory (Zhuhai), Zhuhai 519000, China

carbohydrates, the phosphoenolpyruvate (PEP) functions as phosphoryl donor for the EI protein and the histidine-containing phosphate carrier (HPr) transmits the phosphate group to the downstream EII proteins, which phosphorylates imported sugars (Deutscher et al. 2006, 2014).

Until now, the notion that carbohydrate metabolism conducts a crucial role in regulating virulence in various bacterial pathogens is becoming an emerging theme. The defective expression of *ptsI* and *crr*, encoding enzyme I and enzyme IIA^{Glc}, reduced the expression of PhoPQ regulon associated with quorum sensing and switched *Salmonella* from growth arrest to acute virulence through activation of virulence factor secretion (Maze et al. 2014; Lim et al. 2019). In *Vibrio cholerae*, PTS modulates virulence gene expression by regulating the expression of *tcpH* and *aphAB* to control the expression of *toxT*, the central activator of virulence gene expression (Wang et al. 2015). A promiscuous man-family PTS transporter of *Streptococcus* exerted influence on SLS-mediated hemolysis and the route of glucose uptake impacting their survivals in human blood (Sundar et al. 2017; 2018). In a mouse model, the impairments in PTS components in *Bacillus anthracis* and *Borrelia burgdorferi* attenuated in vivo virulence via affecting the expression of their master virulence regulators, respectively (Khajanchi et al. 2016; Bier et al. 2020). However, the mechanisms underlying that the specific phosphotransfer reactions mediated by individual sugar-specific PTS branches or components are integrated into a global virulence program to control bacterial pathogenesis remain elusive.

Edwardsiella piscicida is an important gram-negative zoonotic pathogen that infects a variety of farmed fish, mainly depending on its type III secretion system (T3SS) and type VI secretion system (T6SS) controlled by two-component system EsrA-EsrB (Leung et al. 2019). Given the sluggish growth in fermented sugars, *E. piscicida* was initially named *E. tarda*, implying that limited PTS sugars can be utilized by *E. piscicida* (Abott and Janda 2006; Wang et al. 2009; Shao et al. 2015). Recently, we revealed that EvrA is a mannose-6-phosphate (Man-6P) sensor that directly activates *esrB* expression to control T3SS production in *E. piscicida* (Wei et al. 2019). How mannose is transported and activated to fulfill virulence regulation is yet unknown.

Here, we identified 23 components predicted for sugar and nitrogen PTS systems in *E. piscicida*. We also systematically defined the distinct genes required for the 5 PTS sugars utilized by the bacterium. Specifically, PtsH not only participated in carbohydrate utilization but also controlled the expression of T3/T6SS genes in *E. piscicida*. Moreover, residues His15 and Ser46, the established sites for PtsH phosphorylation, showed redundancy in modulating virulence gene expression. In addition, PtsH while not Fpr played a role in modulating virulence gene expression. Finally, PtsH potentiated and transformed mannose to Man-6P to activate virulence regulator EvrA, augmenting virulence gene expression. Collectively, our findings provide new insights into the roles of PtsH in coordination between carbohydrate metabolism and the virulence gene expression of *E. piscicida*.

Materials and methods

Bacterial strains and culture conditions

The strains and plasmids used in this study are shown in Table S1. *E. piscicida* EIB202 and WTΔP, the wild-type strain cured of its endogenous Cm and Str resistance plasmid pEIB202 (Wang et al. 2009), were used as the parental strains for the construction of the in-frame deletion mutant strains (Supplemental Table S1). *E. piscicida* strains were grown in Luria–Bertani broth (LB) or on LB plates (Oxoid, England) and in Dulbecco's modified Eagle's medium (DMEM) (Invitrogen, USA) at 30 °C. DMEM was used to induce T3/T6SS production as well as to yield auto-aggregation phenotypes mimicking in vivo conditions (Zheng et al. 2005). When required, antibiotics were supplemented at the following concentrations: colistin (Col, 16.7 μg/mL), ampicillin (Amp, 100 μg/mL), and kanamycin (Km, 25 μg/mL).

Construction of deletion mutants and complemented strains

In-frame deletion mutants were generated using *sacB*-based allelic exchange (Yin et al. 2018). Overlap PCR was used to generate appropriate DNA fragments for creating in-frame deletions in each target gene. The fragments were inserted into the suicide vector pDM4 with Gibson assembly (Gu et al. 2016) and the resulting plasmids were introduced into *Escherichia coli* SM10 *λpir* for conjugation into *E. piscicida* EIB202 or WTΔP. Transconjugants were selected on LB plates containing Km and Col. Double-crossover events were subsequently selected on LB plates containing 12% sucrose. The fragments containing the corresponding ORF region and putative promoter region were cloned into plasmid pUTt to obtain complementation strains (Yin et al. 2018). All newly constructed plasmids were verified by sequencing. All primers used in this study are listed in Supplemental Table S2.

PTS transport analysis

The PTS-related metabolic pathways were predicted on Kyoto Encyclopedia of Genes and Genomes (KEGG) with default parameters (https://www.genome.jp/kegg/pathway.html). The PTS components were further identified using the BlastN algorithm (NCBI) based on their corresponding homologous sequences. Overnight cultures were grown

in LB medium at 30 °C for 24 h. Subsequently, 1% (v/v) inoculum of all *E. piscicida* cultures was inoculated in M9 medium with or without indicated carbohydrates. The M9 medium does not contain any carbohydrates, leading to the growth deficiency of *E. piscicida* strains. The initial pH of the M9 medium with 0.5% (w/v) various sugars was 7.27 ± 0.07. Bromothymol blue (0.1% w/v, Sigma-Aldrich) was used as a pH indicator of sugar fermentation.

Determination of growth curve

Growth curves were determined by Bioscreen C (Oy Growth Ab Ltd, Finland). All *E. piscicida* strains were inoculated into LB for overnight culture and then diluted into fresh LB or DMEM at an OD_{600} of ~ 0.1. Two hundred microliter cultures were transferred into a 100-well plate and then statically cultured at 30 °C. The non-inoculated LB or DMEM were used as a control and all measurements ($n = 6$) were repeated at least three times in independent experiments.

Total RNA extraction and qRT-PCR

E. piscicida strains were statically cultured in DMEM. RNA samples were extracted with a commercial RNA isolation kit (Tiangen, China) and mRNA was reverse-transcribed into cDNA using the FastKing RT kit (Tiangen, China). qRT-PCR was performed with an Applied Biosystems 7500 cycler (Applied Biosystems, USA) with triplicate reactions for each sample. The comparative C_T ($2^{-\Delta\Delta CT}$) method (Gu et al. 2016) was used to quantify the relative levels of each transcript with the specific primer pairs (Table S2) and *gyrB* gene was used as an internal control (Yin et al. 2018).

RNA-seq

For the preparation of mRNA for RNA-seq, the Ribo-Zero-rRNA kit (Epicentre, USA) was initially used to remove rRNA from the RNA samples. The final concentration of RNA samples was determined with a Qubit 2.0 Fluorometer (Thermo Fisher, USA). The VAHTS Stranded mRNA-seq Library Prep Kit for Illumina (Vazyme, China) was used to construct strand-specific RNA-seq libraries, and sequencing was conducted on an Illumina HiSeq 2500 platform, yielding the paired-end reads. Adapter sequences and low-quality bases (PHRED quality scores ≤ 5) were trimmed with the Trimmomatic package (Bolger et al. 2014) using the default parameters and reads smaller than 35 bp were discarded. The RNA-seq data processing procedures and statistical analysis were performed (Tjaden 2015).

SDS-PAGE and western blotting analysis

Whole cell proteins (WCPs) and extracellular proteins (ECPs) were extracted and concentrated (Yin et al. 2018). Overnight cultures of *E. piscicida* were sub-cultured into 50-mL fresh DMEM and statically incubated for 24 h to 72 h at 28 °C; bacteria were then harvested by centrifugation at 5,000 × g for 10 min at 4 °C for WCPs. For ECPs, culture supernatants were filtered with 0.22-μm filters (Millipore, USA), and concentrated using 10 kDa cutoff centrifugal filter devices (Millipore, USA). Proteins were separated by 12% SDS-PAGE, followed by Coomassie blue staining. For western blots, separated proteins were wet transferred onto PVDF membranes (Millipore, USA) and incubated with a 1:1000 dilution of mouse anti-EseB (GL Biochem, China). HRP-conjugated anti-mouse IgG (Santa Cruz Biotechnology, CA) was used at a 1:2,000 dilution as a secondary antibody. Proteins were visualized with TMB substrate (Amresco, USA). Mouse anti-DnaK (Santa Cruz Biotechnology, USA) was used as a loading control.

Animal survival and competitive index assays

Turbot experiments were performed according to protocols approved by the Animal Care Committee of the East China University of Science and Technology (2,006,272) and the Experimental Animal Care and Use Guidelines from the Ministry of Science and Technology of China (MOST-2011–02). Healthy turbot weighing 30.0 ± 3.0 g (~ 2 months old and ~ 1:1 female to male) were obtained from a commercial farm (Yantai, China) and acclimatized with a continuous flow of seawater for 7 days at 16 °C. For fish survival assays, overnight cultures were harvested by centrifugation at 8,000 × g for 2 min at 4 °C and washed three times with phosphate-buffered saline (PBS, pH 7.4). A total of 5.0×10^4 colony-forming units (CFUs) bacteria suspended in PBS were injected into each fish via the intraperitoneal (i.p.) route and PBS was used as a negative control. A total of 30 fish were injected with each strain and fish mortality was monitored daily. The infection experiments were performed at least three independent times.

Competitive index (CI) assays were performed between WT, or the indicated gene-deletion mutant strains, and WTΔp, the WT strain cured of its endogenous Cm and Str resistance plasmid pEIB202 (Wang et al. 2009). Inocula were prepared using fresh cultures of bacteria that were diluted and mixed at a 1:1 ratio. A total of ~ 10^5 CFUs bacteria in a 100 μL inoculum were i.p. injected into each fish. At 8-day post-injection (DPI), the livers from fish in each group (6 fish/group) were collected, homogenized, and plated on LB plates with or without the presence of Cm to distinguish WT Δp (Cm^s) from other strains (Cm^r) (Yang et al. 2017).

The ratios of the bacterial counts were used to determine CI values.

Statistical analysis

GraphPad Prism (version 8.0) was used for the statistical analyses. Data are presented as the mean ± SD of triplicate samples per experimental condition unless otherwise noted. Statistical analyses were performed using unpaired two-tailed Student's *t* test for the metabolite level analysis, one-way ANOVA analyses followed by Bonferroni's multiple-comparison post-test comparing the data of CI values, or Kaplan–Meier survival analysis with a log-rank test. Differences were considered significant at $*P < 0.05$, $**P < 0.01$, and $***P < 0.001$.

Results

Identification of the PTS components and cognate PTS sugars in E. piscicida

Edwardsiella genus bacterium was initially given the name "tarda" to describe its weak ability of sugar fermentation and the genetic basis underlying this phenotype remains unknown. Bioinformatics analysis with KEGG indicated that *E. piscicida* EIB202 encodes 23 PTS components (Wang et al. 2009). Similarly, all the currently known *Edwardsiella* species encode very few PTS genes (24 for *E. ictaluri*, 29 for *E. anguillarum*, 28 for *E. tarda*, and 36 for *E. hoshinae*) as compared to other enteric pathogens, e.g., 58 for *Salmonella* Typhimurium LT2 and 52 for *E. coli* O157:H7 EDL933. KEGG entry etr02060 informed that *E. piscicida* encodes 20 genes for sugar PTS and 3 for nitrogen PTS (PTS^{Ntr}), respectively, including one protein for EI, 2 for HPrs, and 7 for EIIs (Fig. 1A and Table 1). Of them, PtsI was supposed to be PEP-related protein phosphotransferase EI and Hpr proteins were annotated to include Fpr for the utilization of fructose, and PtsH supporting the transport of the rest of sugars. A total of 7 saccharides were predicted as the cognate potential PTS sugars including glucose (Glc), fructose (Fru), mannose (Man), N-acetylglucosamine (GlcNAc), N-acetylgalactosamine (GalNAc), L-ascorbic acid (LAc), and β-glucoside (β-Glu).

Functional analysis of PTS components respective PTS sugar transport in E. piscicida

To verify the utilization of putative PTS sugars, the WT strain was inoculated into M9 medium with the corresponding saccharides (Fig. 2A). Ascorbyl glucoside (AGlu) was used as the β-glucoside carbon source substrate. The growth

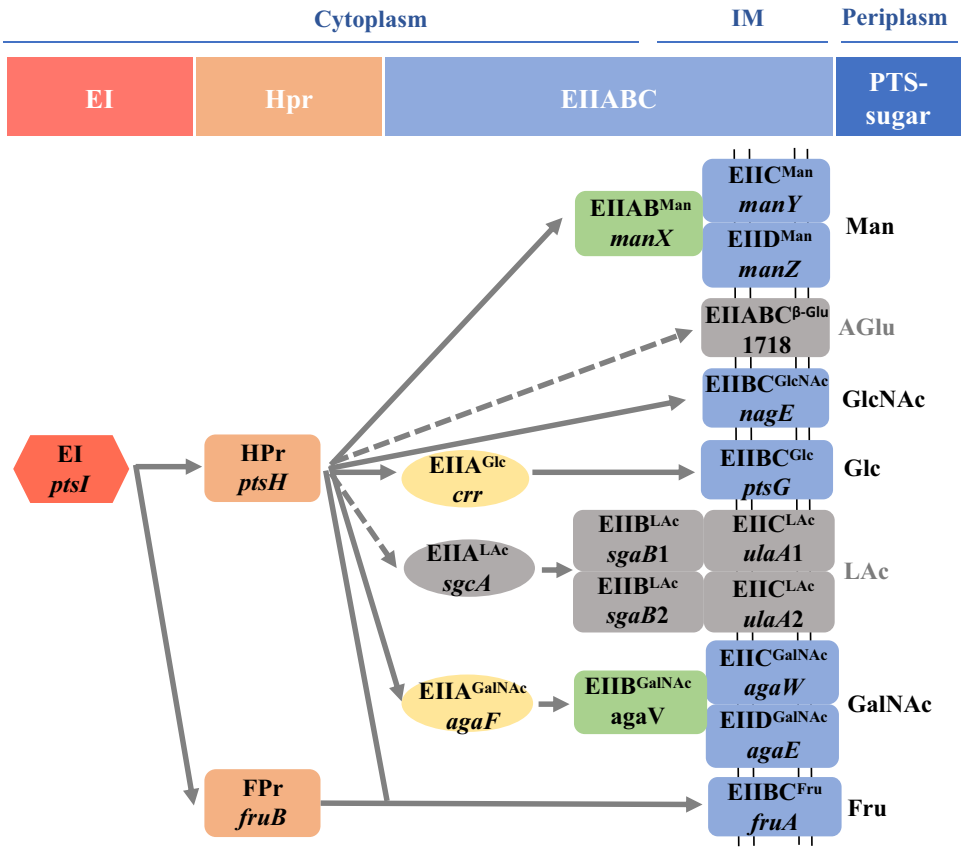

Fig. 1 The schematic of PTS systems and PTS sugars in *E. piscicida*. Predicted PTS components and their corresponding PTS sugars. The dashed lines and the corresponding saccharides marked in gray indicated that L-ascorbate (LAc) and ascorbyl glucoside (AGlu) could not be efficiently utilized by *E. piscicida*

Table 1 Putative PTS components and PTS sugars in *Edwardsiella piscicida* EIB202

Family	Saccharide	Component	Gene	Annotation
EI		EI (PtsI)	ETAE_1131 *ptsI*	Phosphoenolpyruvate-protein phosphotransferase (PEP EI)
HPr		HPr (PtsH)	ETAE_1132 *ptsH*	Phosphohistidinoprotein-hexose phosphotransferase component
	Fructose	FPr	ETAE_2303 *fruB*	Fructose-specific PTS HPr component
EII	Fructose	EII BC^{Fru}	ETAE_2301 *fruA*	Fructose-specific PTS system IIBC component
	Glucose	$EIIA^{Glc}$	ETAE_1130 *crr*	Glucose-specific PTS system enzyme IIA
		$EIIBC^{Glc}$	ETAE_2090 *ptsG*	Glucose-specific PTS system enzyme IIBC subunit
	L-Ascorbic acid	$EIIA^{LAc}$	ETAE_3026 *sgcA*	Putative phosphotransferase enzyme IIA component SgcA
		$EIIB^{LAc}$ 1	ETAE_3027 *sgaB*1	Phosphotransferase enzyme IIB component
		$EIIB^{LAc}$ 2	ETAE_3293 *sgaB*1	L-Ascorbic acid-specific enzyme IIB component of PTS
		$EIIC^{LAc}$ 1	ETAE_3028 *ulaA*1	Ascorbate-specific PTS system enzyme IIC
		$EIIC^{LAc}$ 2	ETAE_3292 *ulaA*2	Ascorbate-specific PTS system enzyme IIC
	Mannose	$EIIAB^{Man}$	ETAE_1559 *manX*	Mannose-specific PTS system enzyme IIAB component
		$EIIC^{Man}$	ETAE_1558 *manY*	Mannose-specific PTS system enzyme IIC subunit
		$EIID^{Man}$	ETAE_1557 *manZ*	Mannose-specific PTS system enzyme IID
	N-Acetylgalactosamine	$EIIA^{GalNAc}$	ETAE_2532 *agaF*	N-Acetylgalactosamine-specific PTS system enzyme IIA
		$EIIB^{GalNAc}$	ETAE_0679 *agaV*	N-Acetylgalactosamine-specific PTS system enzyme IIB
		$EIIC^{GalNAc}$	ETAE_2534 *agaW*	N-Acetylgalactosamine-specific PTS system enzyme IIC
		$EIID^{GalNAc}$	ETAE_2533 *agaE*	N-Acetylgalactosamine-specific PTS system enzyme IID
	N-Acetylglucosamine	$EIIBC^{GlcNAc}$	ETAE_2616 *nagE*	N-Acetylglucosamine-specific PTS system enzyme IIBC subunit
	β-Glucoside	$EIIABC^{β-Glu}$	ETAE_1718	β-Glucoside-specific PTS system enzyme IIABC

of WT in M9 medium alone and M9 supplemented with AGlu and LAc was severely low, suggesting that β-glucoside and L-ascorbic acid could not be efficiently utilized by *E. piscicida*. Glucose, fructose, mannose, N-acetylglucosamine, and N-acetylgalactosamine enabled the growth of WT (Fig. 2A).

In order to further define the roles of PTS components in specific sugar transport, we set out to systematically construct the in-frame deletion mutants of them. In total, 16 in-frame deletion mutants of predicted sugar PTS system components were successfully constructed and yet we failed to obtain the deletion mutants of the essential genes *ptsG* (EII B^{Glc}), *crr* (EII A^{Glc}), *agaV* (EII B^{GlcNAc}), and *ETAE_1718* (EII $A^{β-Glu}$) (Table S1). The growth of these PTS-associated mutants in M9 medium supplemented with glucose or other PTS sugars was assayed (Fig. 2A–B). The growth of Δ*ptsI* was severely impaired in the presence of all saccharides (Fig. 2A–B, Table 1), validating its essential role as the sole EI in PEP phosphorylation cascade. In contrast, two PTS^{Ntr} mutant strains, Δ*ptsP* and Δ*npr*, showed efficient growth in M9 plus glucose medium, suggesting their roles are irrelevant to PTS sugar utilization (Fig. 2B). Except grown in the M9 plus fructose medium, Δ*ptsH* strain exhibited significantly decreased growth in all the rest of tested PTS sugars. Consistent with this, the Δ*fruB* strain with the putative FPr disrupted showed significantly decreased growth in fructose while the Δ*ptsH*Δ*fruB* double deletion strain exhibited drastically impaired growth in this medium, demonstrating their redundancy roles in supporting fructose transport (Fig. 2A) (Deutscher et al. 2014).

In addition, other in-frame deletion mutants of distinct EII components showed well growth comparable to that of WT (Fig. 2B) and only exhibited deficient growth when their corresponding PTS sugars were supplemented as the sole carbon sources (Table 2), validating that *manXYZ* operon was responsible for the utilization of mannose and *agaW/agaE* were involved in the utilization of N-acetylglucosamine. Intriguingly, the deletion of *manZ* also resulted in the impaired growth of *E. piscicida* under glucose supplementation in M9 medium (Table 2 and Fig. 2B), suggesting a promiscuous role of *manZ* for glucose uptake. Taken together, these data indicated the respective functions of the PTS components in PTS sugars utilization.

ptsH and manZ disruption decreases T3SS protein level of E. piscicida

We further measured the growth of all the 18 deletion mutants in glucose-supplemented DMEM mimicking intracellular conditions. Similarly, Δ*ptsI* growth was also severely impaired in this condition (Table 2). Δ*ptsH* and Δ*manZ* exhibited severe growth retardation in this glucose-containing DMEM (Fig. 3A–B, Table 2). The $ptsH^+$ and $manZ^+$ complement strains rescued their growth as that of WT (Fig. 3A–B). However, there were no growth defects in Δ*ptsH* and Δ*manZ* compared to that of WT in nutrient-rich

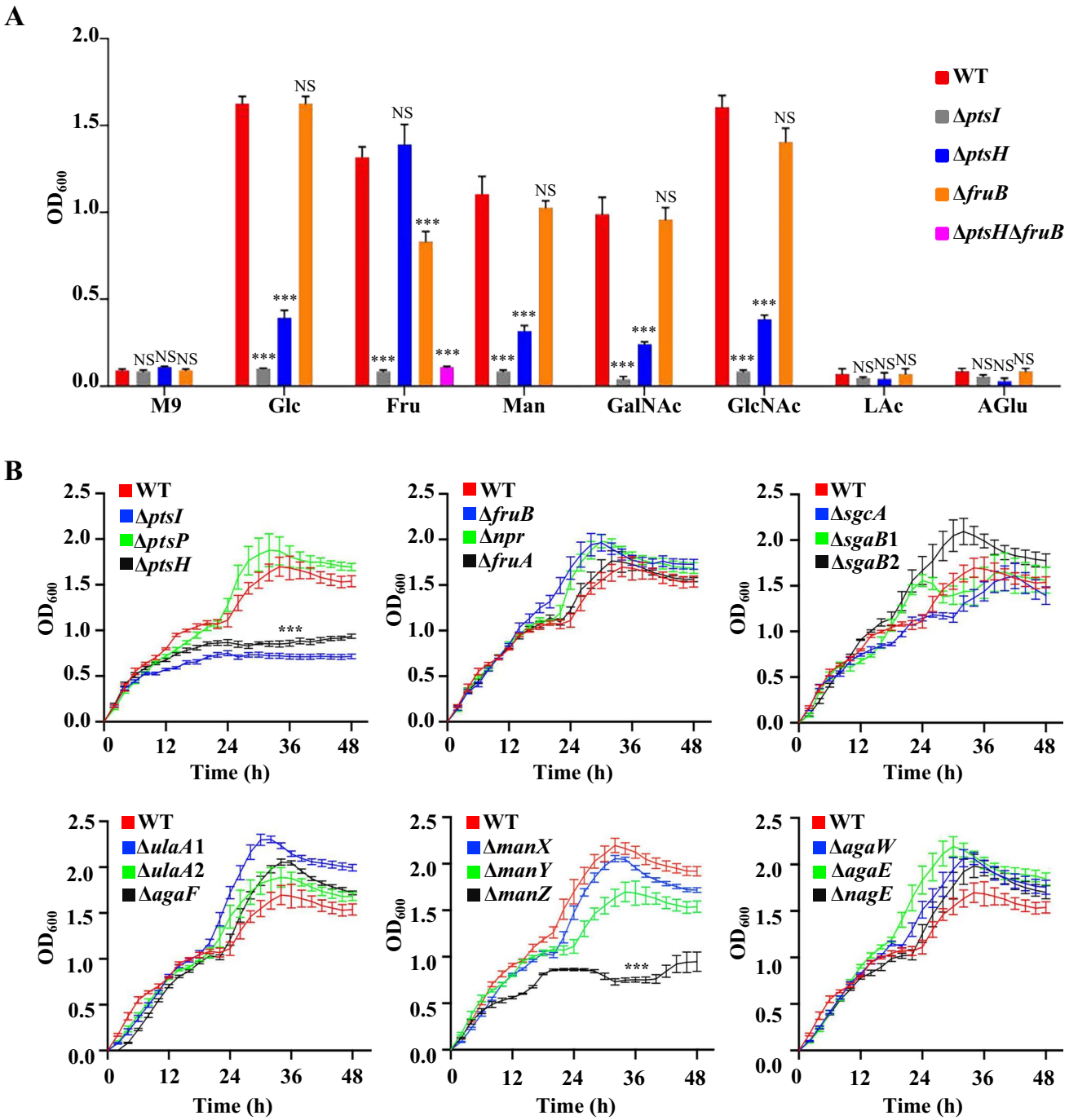

Fig. 2 Growth of the wild-type EIB202 (WT) and PTS mutant strains in M9 medium supplemented with defined sugars. **A** Growth of the WT and Δ*ptsH* strain inoculated in M9 medium supplemented with 5 mg/mL of indicated PTS sugars, including glucose (Glc), fructose (Fru), mannose (Man), N-acetylgalactosamine (GalNAc), N-acetylglucosamine (GlcNAc), L-ascorbate (LAc), and ascorbyl glucoside (AGlu). The OD_{600} values of bacterial cultures were measured at 24-h post-inoculation. The results are shown as the mean ± S.D. ($n = 6$). ***$P < 0.001$, NS, not significant ($P > 0.05$), based on the student's *t* test in comparison to WT. **B** Growth curves of 18 deletion mutants of PTS system components grown in M9 medium supplemented with 5 mg/mL glucose as the sole carbon source. The results are shown as the mean ± S.D. ($n = 6$)

medium LB (Table 2). Collectively, PtsH and ManZ seem to play important roles for growth in intracellular conditions in *E. piscicida.*

We further explored whether carbohydrate metabolism influences the pathogenesis of *E. piscicida.* Due to the appearance of EseB-mediated protein filament, T3SS

Table 2 Functional analysis of in-frame deletion mutants of all predicted PTS components

Strains	M9								LB	DMEM
	/	Glc	Fru	Man	GlcNAc	GalNAc	LAc	AGlu		
EIB202 ΔP	-	+ +	+ +	+ +	+ +	+ +	-	-	+ +	+ +
Δ*ptsI*	-	-	-	-	-	-	-	-	-	-
Δ*ptsP*	-	+ +	+ +	+ +	+	+ +	-	-	+ +	+ +
Δ*ptsH*	-	+	+ +	-	-	-	-	-	+ +	+
Δ*fruB*	-	+ +	+	+ +	+	+ +	-	-	+ +	+ +
Δ*npr*	-	+ +	+ +	+ +	+	+ +	-	-	+ +	+ +
Δ*fruA*	-	+ +	+ +	+ +	+	+ +	-	-	+ +	+ +
Δ*sgcA*	-	+ +	+ +	+ +	+	+ +	-	-	+ +	+ +
Δ*sgaB* 1	-	+ +	+ +	+ +	+	+ +	-	-	+ +	+ +
Δ*sgaB* 2	-	+ +	+ +	+ +	+	+ +	-	-	+ +	+ +
Δ*sgaT* 1	-	+ +	+ +	+ +	+	+ +	-	-	+ +	+ +
Δ*sgaT* 2	-	+ +	+ +	+ +	+	+ +	-	-	+ +	+ +
Δ*manX*	-	+ +	+ +	-	+	+	-	-	+ +	+ +
Δ*manY*	-	+ +	+ +	-	+	+ +	-	-	+ +	+ +
Δ*manZ*	-	+	+ +	-	+	+ +	-	-	+ +	+
Δ*agaF*	-	+ +	+ +	+ +	-	+ +	-	-	+ +	+ +
Δ*agaW*	-	+ +	+ +	+ +	-	+ +	-	-	+ +	+ +
Δ*agaE*	-	+ +	+ +	+ +	-	+ +	-	-	+ +	+ +
Δ*nagE*	-	+ +	+ +	+ +	+	+ +	-	-	+ +	+ +

Strains were cultured in LB, DMEM, M9, or M9 with 0.5% (w/v) predicted PTS sugars for 24 h. Glucose (Glc), fructose (Fru), mannose (Man), N-acetylgalactosamine (GalNAc), N-acetylglucosamine (GlcNAc), L-ascorbate (LAc), and ascorbyl glucoside (AGlu)

production could be assessed by auto-aggregation phenotype in *E. piscicida* (Gao et al. 2015). Δ*ptsI* was not considered in the following experiments owing to its poor growth in DMEM. Intriguingly as Δ*T3SS* and Δ*esrB* did, Δ*ptsH* and Δ*manZ* exhibited marked deficiency in auto-aggregation, whereas other mutants possessed similar auto-aggregation phenotypes as WT did (Fig. 2C). Consistent with the auto-aggregation phenotypes, the reduced amounts of extracellular T3SS proteins were observed in Δ*ptsH* and Δ*manZ* as confirmed by western blot analysis against EseB (Fig. 2D).

PtsH modulates T3/T6SS gene expression as revealed by RNA-seq

We further utilized RNA-seq to compare the transcriptomes of Δ*ptsH* and WT cells grown in DMEM. Differential transcriptomics analyses indicated 163 differentially expressed genes in Δ*ptsH* compared to those in WT ((|log2(FC)|> 1 and $P < 0.05$) (Fig. 4A, Supplemental Table S3). Specifically, the expressions of 36 genes were down-regulated and the expressions of 127 genes were up-regulated. With regard to virulence genes, almost all of the T3/T6SS genes ($n = 49$) had significantly lower transcript levels in Δ*ptsH* than those in WT (Fig. 4A–B). Consistent with the crucial role of PtsH in carbohydrate metabolism, the PtsH-regulated genes were mainly grouped into "energy production and conversion," "amino acid transport and metabolism," and "carbohydrate transport and metabolism" (Fig. 4C). Subsequently, we set out to detect transcript levels of established virulence regulatory genes (*esrA*, *esrB*, and *esrC*), T3SS genes (*eseB*, *eseC*, and *eseD*), and T6SS genes (*evpP*, *evpC*, and *evpI*) by qRT-PCR assays. Due to the absence of *ptsH*, T3/T6SS gene transcripts significantly declined compared to those in WT, whereas no apparent changes were found in the transcript levels of virulence regulators EsrA/B/C (Fig. 4D). These results demonstrated PtsH's function in controlling not only the carbohydrate metabolism but also the expression of virulence determinants.

Phosphorylation of PtsH is involved in the regulation of T3SS yields

The complement of *ptsH* could fully restore the auto-aggregation and T3/T6SS production in Δ*ptsH* (Fig. 5A–B), demonstrating that PtsH modulates the expression of T3/T6SS genes. As a histidine-containing phosphocarrier protein, HPr is generally phosphorylated at the active site residues, i.e., histidine 15 (His15) and serine 46 (Ser46) (Waygood 1998; Marquez et al. 2002). In PtsH, His15 ~ P and Ser46 ~ P were previously established to be involved in PTS sugar utilization and bacterial virulence regulation, respectively (Deutscher et al. 2005;

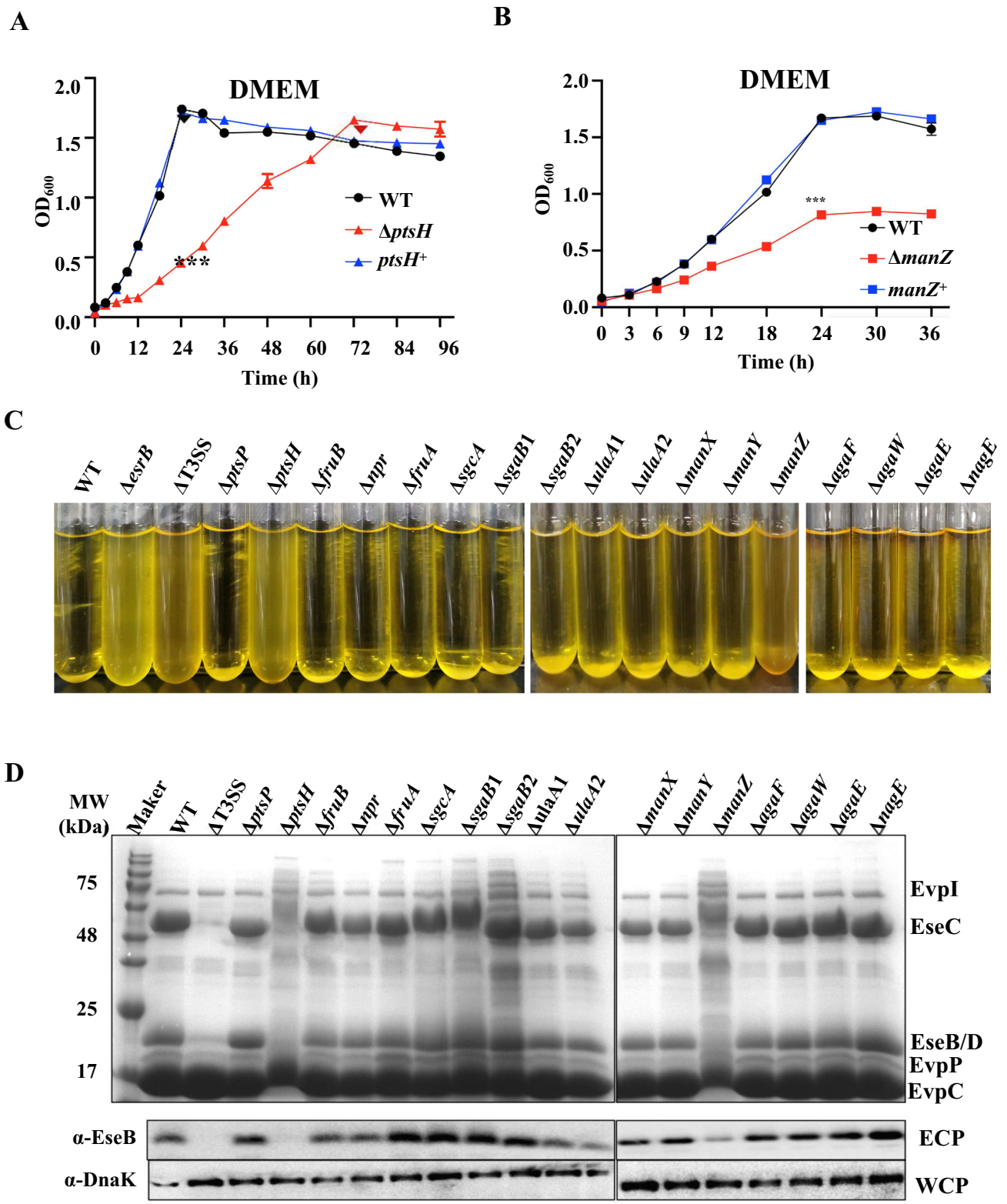

Fig. 3 PtsH and ManZ are essential for the T3SS yields in *E. piscicida* cells grown in DMEM. **A–B** Growth curve of WT, Δ*ptsH*, ΔmanZ, *ptsH*$^+$, and *manZ*$^+$ strains grown in DMEM. The OD_{600} values of indicated cultures were measured at the indicated time point post-inoculation. Results were shown by the mean ± SD ($n = 6$). **C** Auto-aggregation in the deletion mutants of putative PTS component genes grown in DMEM supplemented with 5 mg/mL glucose. **D** Extracellular protein profiles (ECP, upper panel) and western blot (lower panel) analysis of EseB and EvpP yields in the indicated mutants. DnaK in the cell lysates (WCP) was used as the loading control. All images are representative of triplicated experiments

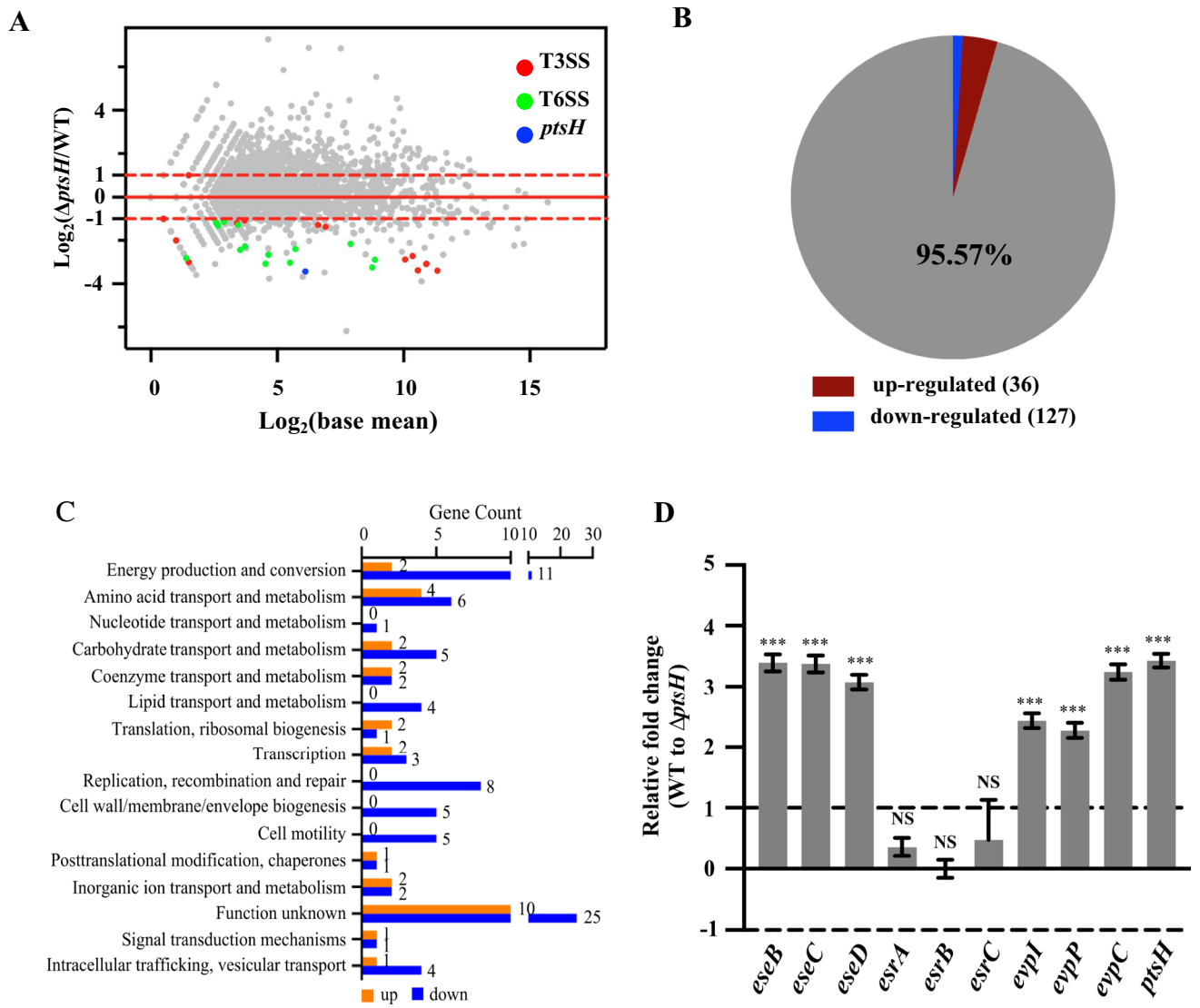

Fig. 4 PtsH is involved in T3/T6SS gene expression. **A** Differential transcriptomics analyses in WT and Δ*ptsH* cells grown in DMEM ($n=3$). The $\log_2$ fold changes of the abundances of each transcript in Δ*ptsH* vs WT cells (*y* axis) were plotted against that of the averaged (Base mean) transcript levels of them (*x* axis). The genes of T3SS (red), T6SS (green), and *ptsH* (blue) are highlighted. **B** Class makeup of the differentially expressed genes identified from the RNA-seq analyses ($n=3$) in Δ*ptsH* relative to WT cells. **C** PtsH is involved in various processes. The number of enriched genes in each category is shown. **D** qRT-PCR analysis of the transcript levels of indicated T3/T6SS genes in Δ*ptsH* to WT cells grown in DMEM. The results are shown as mean ± SEM ($n=3$), ***$P<0.001$, NS, not significant, based on the student's *t* test. *gyrB* was used as the internal control

Casabon et al. 2009). To explore the crucial amino acid residue of PtsH contributing to the T3SS production, PtsH variants, i.e., H15A, S46A, H15A/S46A, D23A/D69A, H15A/D32A/D69A, and H15A/D32A/S46A/D69A, were expressed in the Δ*ptsH strain*. The alanine substitutions of residues aspartic acid 32 as well as 69 (D23A/D69A) were used as negative controls (Fig. 5C). The variants containing both H15A and S46A, i.e., $PtsH^{H15A/S46A}$ and $PtsH^{H15A/D32A/S46A/D69A}$, exhibited deficient T3/T6SS production similar to that of Δ*ptsH* (Fig. 5B–C), while other PtsH variants including the single substitution of H15A or S46A possessed similar extracellular protein profiles comparable to that of WT. Additionally, we sought to determine the transcript levels of T3SS genes (*eseB*, *eseC*, and *eseD*) and T3SS regulatory genes (*esrA* and *esrB*) in the indicated strains expressing PtsH variants. Congruent with the extracellular protein profiles, the significantly decreased T3SS gene transcripts were identified in strains harboring substitutions of both H15A and S46A, further indicative of the requirements of phosphorylation in both His15 and Ser46 for the modulation of T3SS expression (Fig. 5D).

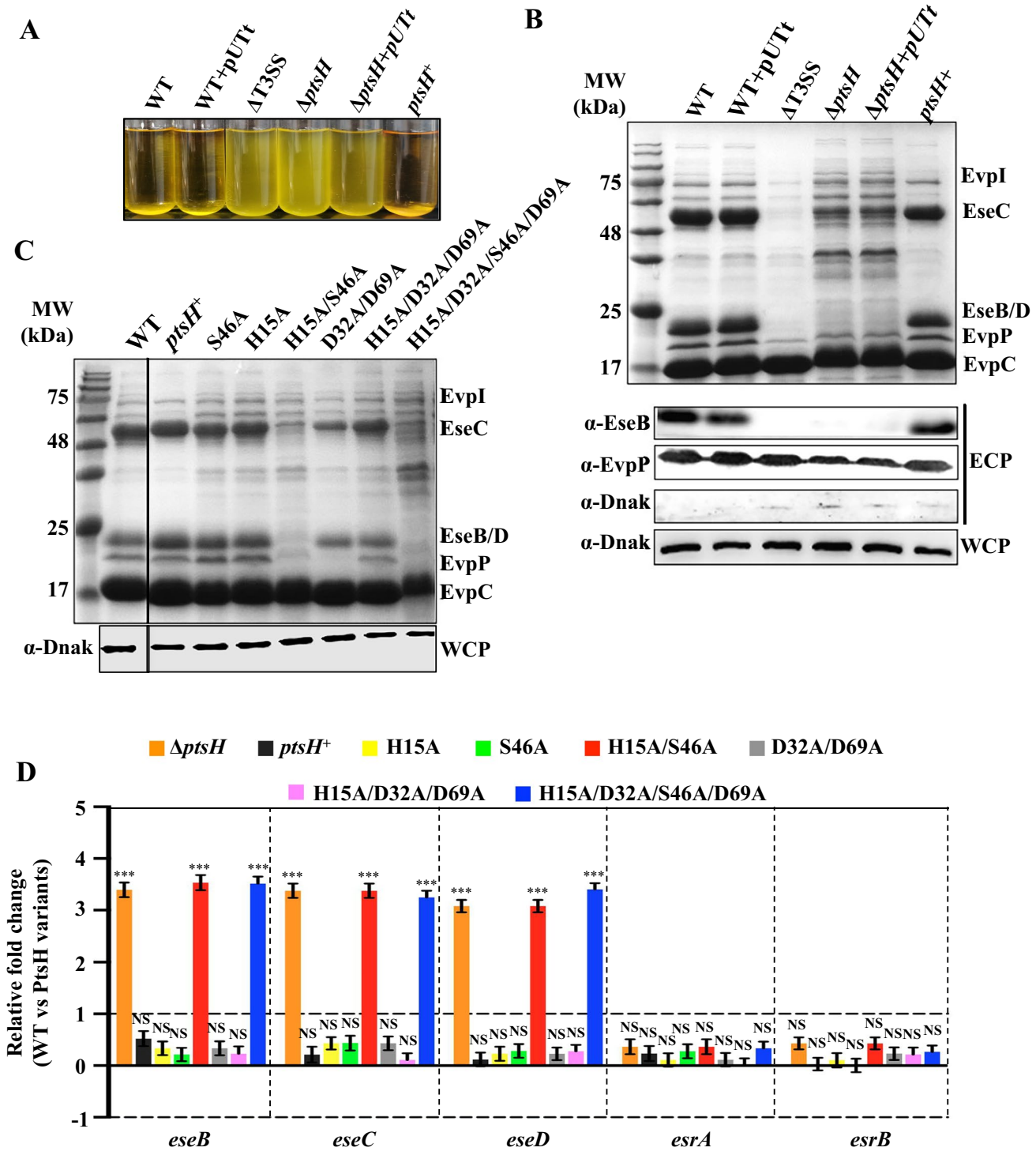

Fig. 5 PtsH phosphorylation at His15 and Ser46 residues is redundant in the activation of T3SS gene expression. **A** Auto-aggregation of Δ*ptsH* and the complement *ptsH*$^+$ strains. The empty plasmid pUTt was introduced into WT or Δ*ptsH* strains as a control. **B–C** ECP profiling (upper panel) and western blot (lower panel) analysis of EseB and EvpP yields in Δ*ptsH* and Δ*ptsH* strains expressing wt PtsH (*ptsH*$^+$) (B), or PtsH variants with substitution in the residues that could not be phosphorylated (C). DnaK in the ECP and WCP was used as the loading control. **D** qRT-PCR analysis of the transcript levels of indicated T3SS genes in WT or Δ*ptsH* cells expressing wt or variants PtsH grown in DMEM. The results are shown as mean ± SEM ($n = 3$), ***$P < 0.001$, NS, not significant, based on the student's *t* test. *gyrB* was used as the internal control

PtsH coordinates mannose utilization and virulence gene expression

Mannose-6-phosphate (Man-6P) was established to bind to virulence regulator EvrA to activate *esrB* expression (Wei et al., 2019). We thus investigated the roles of mannose utilization in mediating virulence towards fish host in *E. piscicida*. Corroborating to our previous findings (Wei et al., 2019), the deletion of *manZ* resulted in impaired auto-aggregation and production of the extracellular T3SS proteins (Fig. 6A and B). The reintroduction of *manZ* fully rescued these defects in Δ*manZ*. In line with these results, the transcript levels of T3SS genes (*eseB*, *eseC*, and *eseD*) and T6SS genes (*evpP*, *evpC*, and *evpI*) were all significantly declined in Δ*manZ* cells grown in DEME supplemented with mannose as compared to that of the WT (Fig. 6C). Moreover, the transcript levels of T3/T6SS genes were significantly augmented in *E. piscicida* cells grown in DMEM supplemented with mannose as compared to that with glucose (Fig. 6D). Mannose modulation of T3SS gene expression also appeared to be dependent on PtsH as the transcript levels of T3SS genes in Δ*ptsH* cells showed no difference between DMEM containing mannose and glucose (Fig. 6D). It was also notable that *ptsH* expression seems not to be affected by mannose, and the expression of *evrA* was up-regulated in response to mannose in WT but not in Δ*ptsH* cells (Fig. 6C–D). Taken together, these data indicated that PtsH and ManZ are essentially involved in mannose utilization, which facilitates virulence gene expression in *E. piscicida*.

A turbot infection model was used to explore PtsH role in controlling virulence in vivo. Δ*ptsH* and Δ*manZ* strains exhibited significantly attenuated virulence. Approximately 70% of fish survived after infection with Δ*ptsH* and Δ*manZ*, while the fish challenged with $ptsH^+$ and $manZ^+$ showed 100% mortalities at 12 DPI, similar to those injected with WT (Fig. 6E). Meanwhile, in vivo CI assays were carried out to explore whether PtsH is required for optimal *E. piscicida* fitness during infection (Fig. 6F) with the Δ*ptsH* and Δ*manZ* related strains and WTΔP, the wild-type strain with pEIB202 cured, proficient in in vivo colonization (Fig. 6F) (Yang et al. 2017). The Δ*ptsH* and Δ*manZ* were significantly impaired in the in vivo competition with WT and the corresponding complement strains, $ptsH^+$ and $manZ^+$ resulted, showed WT level of colonization. Collectively, these data demonstrated that PtsH and ManZ are critical for *E. piscicida* optimal growth in vivo.

Discussion

E. piscicida has been increasingly recognized to be a huge threat to the world's aquaculture industries. To elucidate the mechanism of the carbohydrate metabolism in *E. piscicida* and its potential relationship to pathogenesis, the PTS sugars utilized by *E. piscicida* the crucial PTS components facilitating the cognate sugar transport were determined in this study. Being the crucial component of PTS, PtsH supported *E. piscicida* to use mannose both as the carbon source for growth and as a specific host signal to trigger virulence program. Specifically, PtsH phosphorylation at His15 and Ser46 was revealed to be critical for extracellular T3SS yields. Additionally, the disruption in *ptsH* impaired the bacterial colonization and infection in fish host. These results further delineated that mannose represents as a crucial metabolic signal during infection (Wei et al. 2019), laying a good foundation for the development of novel therapeutics against bacterial infection.

In this work, we systematically defined the genetic basis for PTS sugar utilization in *E. piscicida*. As a versatile zoonotic pathogen threatening various piscine hosts as well as humans, it is a counterintuition that the bacterium encodes paucity of genetic resources for saccharides uptake. Comparative genomic analysis also discerned that *E. piscicida* significantly differs from other Enterobacteriaceae bacteria with the lowest ratio of gene contents related to carbohydrate transport and metabolism (G), reflecting that the organism may be well adapted to the aquatic ecosystems and intracellular niches, where may exist relatively mean carbohydrates (Wang et al. 2009; Yang et al. 2012; Leung et al. 2022). However, we might have underestimated the genetic flexibility of *E. piscicida* in dealing with carbohydrate utilization. An example come up with the observation that Δ*ptsH* also showed marginal growth using glucose, mannose, N-acetylglucosamine, and N-acetylgalactosamine as the sole carbon source, respectively (Fig. 2A), suggesting compensatory pathways have been evolved for fermentation of these PTS sugars. Indeed, *E. piscicida* encodes *ETAE_1144* and *ETAE_2966* for a galactose permease (GalP) and a glucose kinase (Glk), respectively, that may support its growth in glucose and other hexoses in the absence of cognate PTS as in *E. coli* (Hernández-Montalvo et al. 2003). Reverse genetics technologies such as using the defined mutant library and transposon insertion sequencing technology (Wei et al. 2019; Yang et al. 2017) might be useful to facilitate the further annotation of genes for defined carbohydrates in *E. piscicida* and other bacteria.

Our data revealed the unexpectedly important role of PtsH in *E. piscicida* virulence. More importantly, His15 and Ser46 were identified as the crucial residues to coordinate T3SS activation (Fig. 4). Unlike the canonical phosphorylation of His15 controlled by PEP, the ATP-dependent phosphorylation of Ser46 requires a specific HPr kinase/phosphorylase (HprK/P), leading to the inhibition of the phosphorylation of His15 in other bacteria. For instance, the phosphorylation of Ser46 of *B. subtilis* retarded the phosphoryl transfer from EI to HPr at least 100-fold (Deutscher

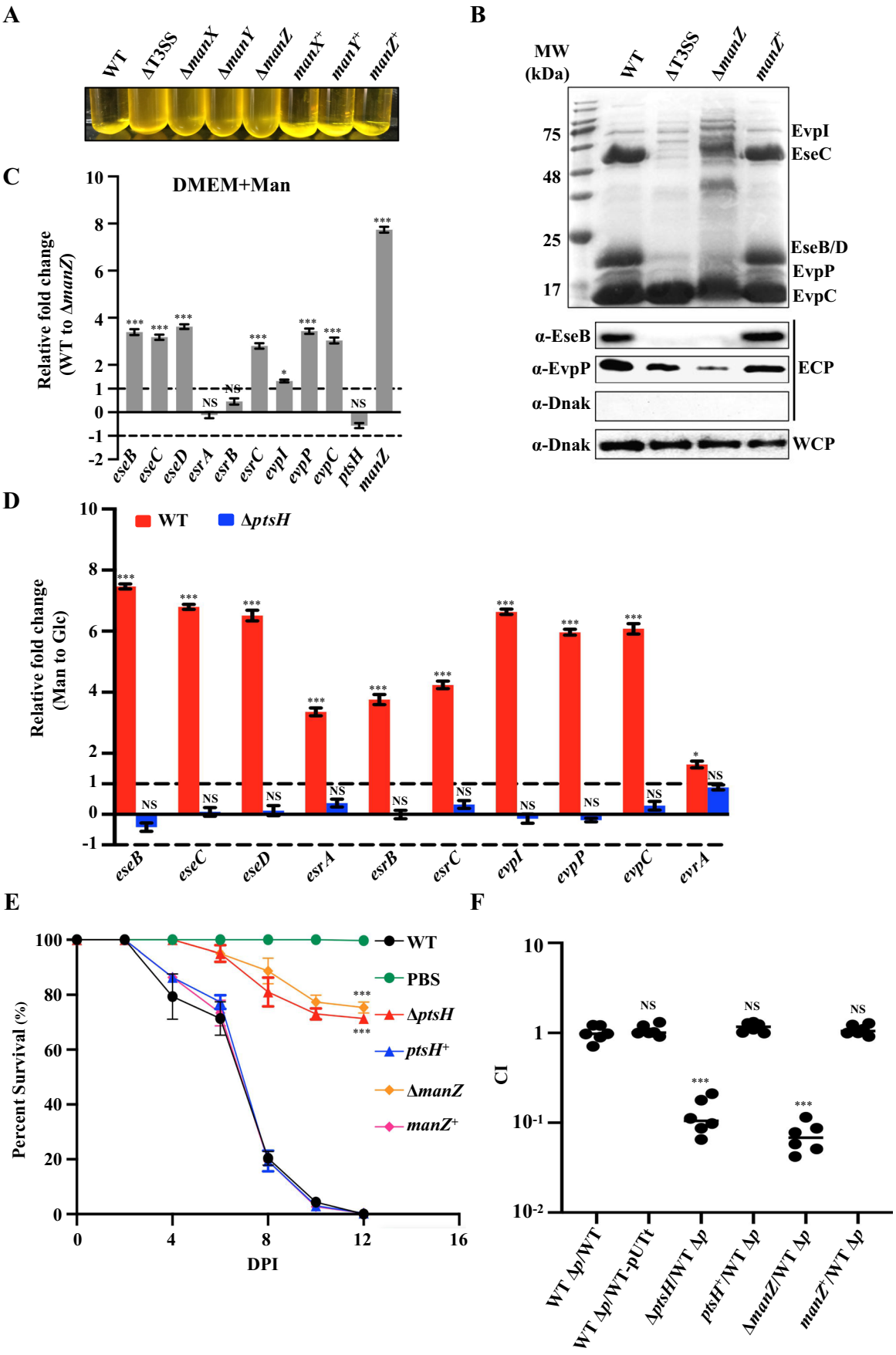
A
WT
ΔT3SS
ΔmanX
ΔmanY
ΔmanZ
manX+
manY+
manZ+
B
MW (kDa)
WT
ΔT3SS
ΔmanZ
manZ+
75
48
25
17
EvpI
EseC
EseB/D
EvpP
EvpC
α-EseB
α-EvpP
α-Dnak
α-Dnak
ECP
WCP
C
DMEM+Man
Relative fold change (WT to ΔmanZ)
eseB
eseC
eseD
esrA
esrB
esrC
evpI
evpP
evpC
ptsH
manZ
D
WT
ΔptsH
Relative fold change (Man to Glc)
eseB
eseC
eseD
esrA
esrB
esrC
evpI
evpP
evpC
evrA
E
Percent Survival (%)
DPI
WT
PBS
ΔptsH
ptsH+
ΔmanZ
manZ+
F
CI
WT Δp/WT
WT Δp/WT-pUTt
ΔptsH/WT Δp
ptsH+/WT Δp
ΔmanZ/WT Δp
manZ+/WT Δp

◂**Fig. 6** PtsH coordinates with ManZ to regulate bacterial virulence in a mannose-dependent manner. **A** Auto-aggregation of WT and mannose (Man) uptake-related mutant strains grown in DMEM supplemented with Man as the sole carbon source. **B** ECP profiling (upper panel) and western blot (lower panel) analysis of EseB and EvpP yields in of WT, Δ*manZ*, and its complement strain *manZ*$^{+}$. DnaK in the ECP and WCP was used as the loading controls. **C** qRT-PCR analysis of the transcript levels of indicated T3/T6SS genes in WT and Δ*manZ* cells grown in DMEM supplemented with 5 mg/mL mannose. The results are shown as mean ± SEM ($n = 3$) and *gyrB* was used as the internal control. **D** qRT-PCR analysis of the transcript levels of indicated T3/T6SS genes in WT (red) and Δ*ptsH* (blue) cells grown in DMEM supplemented with 5 mg/mL mannose compared with those with 5 mg/mL glucose. **E** Survival curves of turbot challenged with the *ptsH* and *manZ* related strains. Phosphate-buffered saline (PBS, pH 7.4) was used as a control. The bacterial strains were suspended in PBS and injected into each turbot at a dose of 5.0×10^4 CFU/fish ($n = 30$ fish/group). Kaplan–Meier survival analysis with a log-rank test is shown. **F** Competition index (CI) assays of equally mixed *ptsH* or *manZ* strains with WTΔp, WT cured of the plasmid pEIB202, in turbot. Data presented are the mean ± SD ($n = 6$). ∗∗∗, $P < 0.001$; NS, not significant, $P > 0.05$, based on ANOVA followed by Bonferroni's multiple-comparison post-test comparing the data to the values from the WTΔp /WT

et al. 2006). Moreover, PtsH/Ser ~ P was supposed to directly or indirectly interact with virulence regulators, thereby providing a link between carbon metabolism and pathogenesis (Deutscher et al. 2005). Our results here supported a model that the PTS-mediated T3SS activation depends on both the level of PEP intermediates and the activities of HPr kinase (Fig. 7), both of which reflect the intracellular ATP level and other physiological states/signals of the cell. Further studies are required to unravel the detailed mechanisms of PtsH's phosphorylation on the virulence of *E. piscicida*.

Since extracellular mannose augments *E. piscicida* virulence in an EvrA-dependent manner (Wei et al. 2019), the loss of ManZ attenuated virulence due to the dysfunction of transportation of extracellular mannose. Given the function of PtsH as the phosphate group carrier to deliver it to enzyme IIC to activate PTS-mannose, Δ*ptsH* is blocked in the import of mannose, leading to the same attenuated virulence as that of Δ*manZ*. The similar virulence phenotype of Δ*ptsH* and Δ*manZ* implied that PtsH and ManZ coordinate *E. piscicida* pathogenicity. Therefore, PtsH and ManZ are indispensable for the enhanced virulence by mannose, which facilitates pathogen sensing of the host environment and triggers virulence programs (Fig. 7). However, our data also support an alternative model in which PtsH might interact with some other factor(s) to facilitate the transfer of phosphoryl group to PTS-mannose complex, which warrants further investigation. Given the essential roles of PtsH in supporting the importation of mannose, the metabolic signal that *E. piscicida* encounters at specific points during infection, and in controlling virulence gene expression by reflecting ATP level and other physiological signals, it could be merited as a valuable gene target for construction of live attenuated vaccines. The same "one stone two bird" strategies have been adopted by using Fur and PhoP that play essential roles in metabolism and virulence regulator as the effective targets for the development of vaccines combating edwardsiellosis infection (Swain et al. 2020, 2022). Taken together, our work deepens our understanding of how bacterial pathogens utilize available sugar to control virulence programs and might be useful for live attenuated vaccine development.

Supplementary Information The online version contains supplementary material available at https://doi.org/10.1007/s00253-022-11848-8.

Author contribution Conceptualization: WQ, SS; data curation: MQQ, JJH; funding acquisition: WQ, SS; investigation: MQQ, JJH, WX, MY; project administration: WQ, SS; supervision: WQ, SS; validation: WQ, SS; visualization: WQ, SS; writing (original draft): SS, MQQ; writing (review and editing): WQ, SS.

Funding This work was supported by grants from the National Natural Science Foundation of China (32130108, 32002436), China Agriculture Research System of MOF and MARA (CARS-47), and the Fundamental Research Funds for the Central Universities (22221062017019).

Data availability All data associated with this study are presented in the main text or supporting information. The raw data of RNA-seq analysis were deposited in NCBI Sequence Read Archive (SRA) database under accession number PRJNA765294.

Declarations

Ethics approval All animal protocols used in this study were approved by the Animal Care Committee of the East China University of Science and Technology (2006272). The Experimental Animal Care and Use Guidelines from Ministry of Science and Technology of China (MOST-2011–02) were strictly followed.

Conflict of interest The authors declare no competing interests.

References

Abbott SL, Janda JM (2006) The Genus Edwardsiella. Prokaryotes 6:72–89

Bier N, Hammerstrom TG, Koehler TM (2020) Influence of the pho sphoenolpyruvate:carbohydrate phosphotransferase system on toxin gene expression and virulence in *Bacillus anthracis*. Mol Microbiol 113:237–252

Boël G, Mijakovic I, Mazé A, Poncet S, Taha MK, Larribe M, Darbon E, Khemiri A, Galinier A, Deutscher J (2003) Transcription regulators potentially controlled by HPr kinase/phosphorylase in Gram-negative bacteria. J Mol Microbiol Biotechnol 5:206–215

Bolger AM, Lohse M, Usadel B (2014) Trimmomatic: a flexible trimmer for Illumina sequence data. Bioinformatics (Oxford, England) 30:2114–2120

Casabon I, Couture M, Vaillancourt K, Vadeboncoeur C (2009) Kinetic studies of HPr, HPr(H15D), HPr(H15E), and HPr(His~P) phosphorylation by the *Streptococcus salivarius* HPr(Ser) kinase/phosphorylase. Biochemistry 48:10765–10774

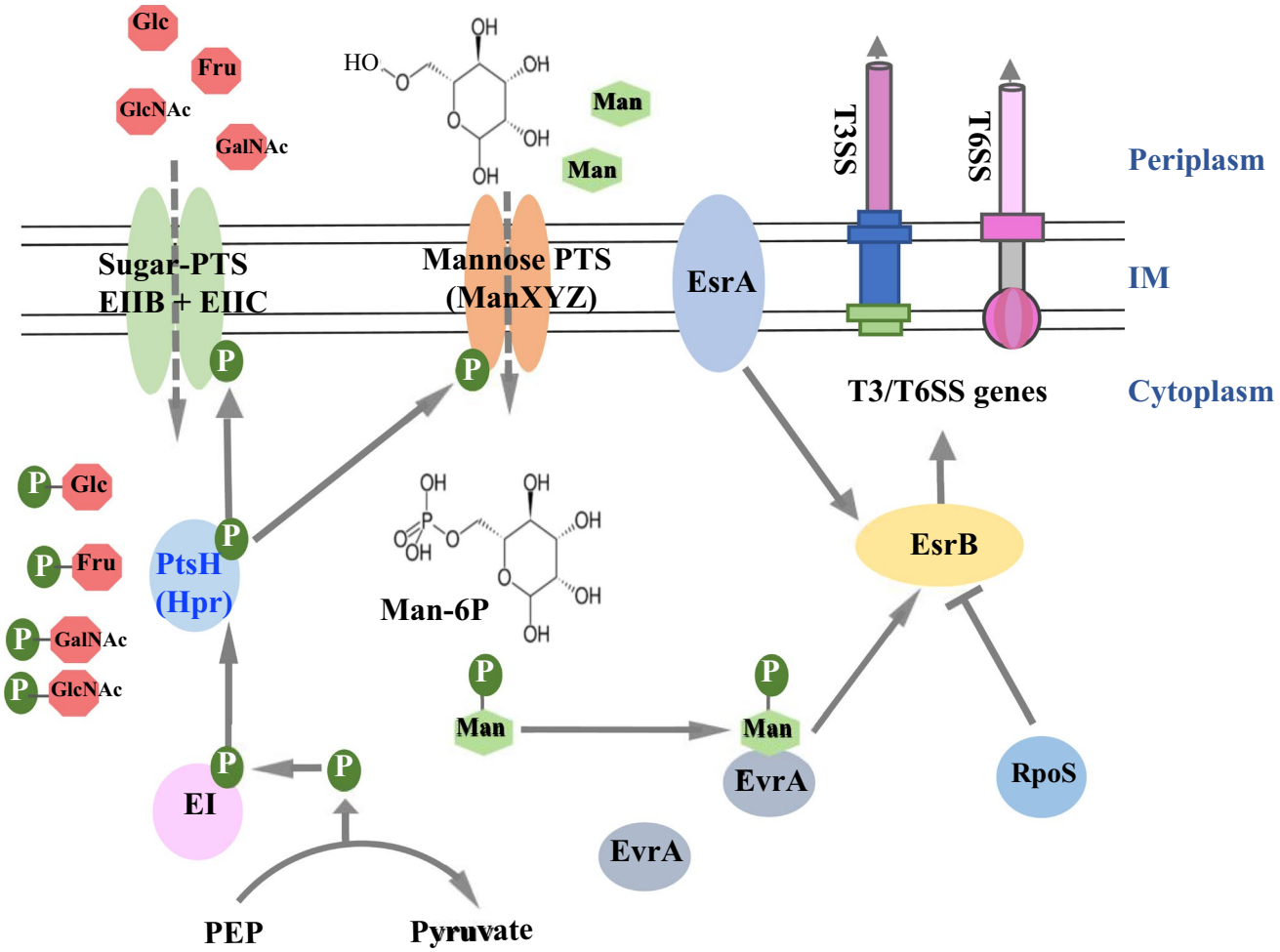

Fig. 7 Schematic of PtsH roles in PTS sugar metabolism and virulence regulation in *E. piscicida*. PEP functions as a donor of the phosphate group and EI autophosphorylates itself followed by transferring the phosphoryl group to PtsH (HPr). PtsH delivers the phosphoryl group to substrate-specific EII, leading to the generation of phosphorylated carbohydrate during uptake. Specifically, mannose is transported into the cytoplasm and transformed as mannose-6-phosphate (Man-6P). Eventually, Man-6P binds to and activates virulence regulator EvrA which in turn further binds the promoter of *esrB* to regulate T3/T6SS

Deutscher J, Herro R, Bourand A, Mijakovic I, Poncet S (2005) P-Ser-HPr–a link between carbon metabolism and the virulence of some pathogenic bacteria. Biochim Biophys Acta 1754:118–125

Deutscher J, Francke C, Postman PW (2006) How phosphotransferase system-related protein phosphorylation regulates carbohydrate metabolism in bacteria. Microbiol Mol Biol Rev 70:939–1031

Deutscher J, Ake FM, Derkaoui M, Zebre AC, Cao TN, Bouraoche H, Kentache T, Milohanic E, Joyet P (2014) The bacterial phosph oenolpyruvate:carbohydrate phosphotransferase system: regulation by protein phosphorylation and phosphorylation-dependent protein-protein interactions. Microbiol Mol Biol Rev 78:232–256

Galinier A, Deutscher J (2017) Sophisticated regulation of transcriptional factors by the bacterial phosphoenolpyruvate: sugar phosphotransferase system. J Mol Biol 429:773–789

Gao ZP, Nie P, Lu JF, Liu LY, Xiao TY, Liu W, Liu JS, Xie HX (2015) Type III secretion system translocon component EseB forms filaments on and mediates autoaggregation of and biofilm formation by *Edwardsiella tarda*. Appl Environ Microbiol 81:6078–6087

Gu D, Liu H, Yang Z, Zhang YX, Wang QY (2016) Chromatin immunoprecipitation sequencing technology reveals global regulatory roles of low cell density quorum-sensing regulator AphA in pathogen *Vibrio alginolyticus*. J Bacteriol 198:516–520

Hernández-Montalvo V, Martínez A, Hernández-Chavez G, Bolivar F, Valle F, Gosset G (2003) Expression of *galP* and *glk* in an *Escherichia coli* PTS mutant restores glucose transport and increases glycolytic flux to fermentation products. Biotechnol Bioeng 83:687–694

Jeckelmann JM, Erni B (2019) Carbohydrate transport by group translocation: the bacterial phosphoenolpyruvate: sugar phosphotransferase system. Subcell Biochem 92:223–274

Jeckelmann JM, Erni B (2020) Transporters of glucose and other carbohydrates in bacteria. Pflugers Arch 472:1129–1153

Khajanchi BK, Odeh E, Gao L, Jacobs MB, Philipp MT, Lin T, Norris SJ (2016) Phosphoenolpyruvate phosphotransferase system components modulate gene transcription and virulence of *Borrelia burgdorferi*. Infect Immun 84:754–764

Leung KY, Wang Q, Yang Z, Siame BA (2019) *Edwardsiella piscicida*: A versatile emerging pathogen of fish. Virulence 10:555–567

Leung KY, Wang QY, Zheng XC, Zhuang M, Yang ZY, Shao S, Achmon Y, Siame BA (2022) Versatile lifestyles of *Edwardsiella*:

free-living, pathogen, and core bacterium of the aquatic resistome. Virulence 13:5–18

Lim S, Seo HS, Jeong J, Yoon H (2019) Understanding the multifaceted roles of the phosphoenolpyruvate: phosphotransferase system in regulation of *Salmonella* virulence using a mutant defective in *ptsI* and *crr* expression. Microbiol Res 223–225:63–71

Liu X, Zeng J, Huang K, Wang J (2019) Structure of the mannose transporter of the bacterial phosphotransferase system. Cell Res 29:680–682

Marquez JA, Hasenbein S, Koch B, Fieulaine S, Nessler S, Russell RB, Hengstenberg W, Scheffzek K (2002) Structure of the full-length HPr kinase/phosphatase from *Staphylococcus xylosus* at 1.95 Å resolution: mimicking the product/substrate of the phospho transfer reactions. Pro Natl Acad Sci U S A 99:3458–3463

Maze A, Glatter T, Bumann D (2014) The carbohydrate metabolism regulator $EIIA^{Glc}$ switches *Salmonella* from growth arrest to acute virulence through activation of virulence factor secretion. Cell Rep 7:1426–1433

Shao S, Lai QL, Liu Q, Wu HZ, Xiao JF, Shao ZZ, Wang QY, Zhang YX (2015) Phylogenomics characterization of a highly virulent *Edwardsiella* strain $ET080813^{(T)}$ encoding two distinct T3SS and three T6SS gene clusters: Propose a novel species as *Edwardsiella anguillarum* sp. nov. Syst Appl Microbiol 38:36–47

Stolz B, Huber M, Markovi-Housley Z, Erni B (1993) The mannose transporter of *Escherichia coli* structure and function of the IIAB-Man subunit. J Biol Chem 268:27094–27099

Sundar GS, Islam E, Gera K, Le Breton Y, Mclver KS (2017) A PTS EII mutant library in group A *Streptococcus* identifies a promiscuous man-family PTS transporter influencing SLS-mediated hemolysis. Mol Microbiol 103:518–533

Sundar GS, Islam E, Braza RD, Silver RD, Le Breton Y, Mclver KS (2018) Route of glucose uptake in the group a *Streptococcus* impacts SLS-mediated hemolysis and survival in human blood. Front Cell Infect Microbiol 8:71

Swain B, Powell CT, Curtiss R 3rd (2020) Pathogenicity and immunogenicity of *Edwardsiella piscicida* ferric uptake regulator (*fur*) mutations in zebrafish. Fish Shellfish Immunol 107:497–510

Swain B, Powell CT, Curtiss R 3rd (2022) Virulence, immunogenicity and live vaccine potential of *aroA* and *phoP* mutants of *Edwardsiella piscicida* in zebrafish. Microb Pathog 162:105355

Tjaden B (2015) De novo assembly of bacterial transcriptomes from RNA-seq data. Genome Biol 16:1

Wang QY, Yang MJ, Xiao JF, Wu HZ, Wang X, Lv YZ, Xu LL, Zheng HJ, Wang SY, Zhao GP, Liu Q, Zhang YX (2009) Genome sequence of the versatile fish pathogen *Edwardsiella tarda* provides insights into its adaptation to broad host ranges and intracellular niches. PLoS One 4:e7646

Wang QY, Millet YA, Chao MC, Sasabe J, Davis BM, Waldor MK (2015) A genome-wide screen reveals that the *Vibrio cholerea* phosphoenolpyruvate phosphotransferase system modulates virulence gene expression. Infec Immun 83:3381–3395

Waygood EB (1998) The structure and function of HPr. Biochem Cell Biol 76:359–367

Wei LF, Qiao HX, Sit B, Yin KY, Yang GH, Ma RQ, Ma JB, Yang C, Yao J, Ma Y, Xiao JF, Liu XH, Zhang YX, Waldor MK, Wang QY (2019) A bacterial pathogen senses host mannose to coordinate virulence. iScience 20:310–323

Yang MJ, Lv YZ, Xiao JF, Wu HZ, Zheng HJ, Liu Q, Zhang YX, Wang QY (2012) *Edwardsiella* comparative phylogenomics reveal the new intra/inter-species taxonomic relationships, virulence evolution and niche adaptation mechanisms. PLoS One 7:e36987

Yang GH, Billings G, Hubbard TP, Park JS, Leung KY, Liu Q, Davis BM, Zhang YX, Wang QY, Waldor MK (2017) Time-resolved transposon insertion sequencing reveals genome-wide fitness dynamics during infection. mBio 8:e1517–e1581

Yin KY, Guan YP, Ma RQ, Wei LF, Liu B, Liu XH, Zhou XH, Ma Y, Zhang YX, Waldor MK, Wang QY (2018) Critical role for a promoter discriminator in RpoS control of virulence in Edwardsiella piscicida. PLoS Pathog 14:e1007272

Zheng J, Tung SL, Leung KY (2005) Regulation of a type III and a putative secretion system in *Edwardsiella tarda* by EsrC is under the control of a two-component system, EsrA-EsrB. Infect Immun 73:4127–4137